

Article

The Effect of Tourmaline on SCR Denitrification Activity of $\text{MnO}_x/\text{TiO}_2$ at Low Temperature

Yizhe Helian, Suping Cui * and Xiaoyu Ma

The Key Laboratory of New Functional Materials of Ministry of Education, College of Materials Science and Engineering, Beijing University of Technology, Beijing 100124, China; helianbjut@163.com (Y.H.); maxiaoyu@bjut.edu.cn (X.M.)

* Correspondence: cuisuping@bjut.edu.cn

Received: 7 August 2020; Accepted: 27 August 2020; Published: 4 September 2020



Abstract: Selective catalytic reduction (SCR) technology is the most widely used flue gas denitration technology at present. The stability of a catalyst is the main factor limiting the development of this technology. In this study, an environmentally friendly and highly efficient NH_3 -SCR catalyst was prepared by coprecipitation method from acidolysis residue of industrial waste and tourmaline. We found that the addition of tourmaline has an important impact on the denitration activity of the catalytic material. The NO_x conversion exceeded 97% at 200 °C with the dosage of 10% tourmaline, which is about 7% higher than that without doping. The improvement of catalytic performance was mostly attributed to the permanent electrodes of tourmaline, which effectively promotes the dispersion of $\text{MnO}_x/\text{TiO}_2$ catalytic materials, increases the number of acidic sites and changes the valence distribution of manganese ions in products, which speeds up the diffusion of protons and ions, resulting in the acceleration of redox reaction. These as-developed tourmaline-modified $\text{MnO}_x/\text{TiO}_2$ materials have been demonstrated to be promising as a new type of highly efficient low-temperature NH_3 -SCR catalyst.

Keywords: tourmaline; permanent electrodes; $\text{MnO}_x/\text{TiO}_2$ catalytic materials; acceleration of redox reaction

1. Introduction

Nitrogen oxides (NOs) are the primary source of environmental problems such as photochemical smog and atmospheric acid deposition, the removal of NO_x is a matter of great urgency. As one of the principal sources of nitrogen oxides emission, cement kilns frequently adopt selective catalytic reduction (SCR) technology to effectively abate flue gas [1]. Catalytic materials are the kernel of SCR technology, thus selecting a suitable catalyst could effectively increase the denitration efficiency and reduce costs [2]. However, on account of the operation of waste heat utilization and flue gas desulfurization, dust removal will lower the flue gas temperature below 200 °C and, accordingly, the traditional catalyst would not meet the requirement [3]. For the past few years, the low-temperature SCR denitration catalyst of the manganese-titanium system has gradually become a research hotspot [4], because of its excellent low-temperature SCR activity and certain anti-sulfur poisoning ability. Previous research of the project group adopted acid hydrolysis residue from the titanium dioxide industry, produced by the sulfuric acid process as raw material, and prepared the $\text{MnO}_x/\text{TiO}_2$ catalyst via co-precipitation method. The initial catalytic activity of the catalyst reaches up to 91%, but the stability is relatively poor; after long-term denitration at 200 °C for ten hours, the catalytic activity drops below 80%. It was discovered that the major reasons for the poor stability of denitration are the integrity of crystallinity, the decrease of specific surface area and the lessening of the acidic sites number after long-term

catalytic reaction. Further improvement of the catalytic performance is the current problem that requires handling.

In consideration of the above problems, this paper considers using non-metallic mineral tourmaline to compound with this kind of catalytic material, and explores the effect of tourmaline on its catalytic activity. Tourmaline is a borosilicate mineral with complex chemical composition and ring structure [5]. Because of its spontaneous permanent electrodes, tourmaline and titanium dioxide are combined to improve the activity of titanium dioxide by using polarization characteristics. It has been widely used in the field of photo-catalysis [6]. The addition of tourmaline can effectively inhibit the recombination of photo-generated electrons and holes in the process of titanium dioxide catalysis, change the symmetry of the Ti–O–Ti bond and change the surface structure of anatase titanium dioxide. There are numerous surface lattice defects to improve the photo-catalytic effect [7]. However, there is no systematic research on the application of tourmaline in the field of thermal denitration catalysis at present. In addition, tourmaline reserves within the scope of exploration are tens of millions of tons, are abundant and are low in price; thus, if it works, the production cost of the catalyst will be greatly reduced compared with the original process. Hence, tourmaline was considered to compound with the $\text{MnO}_x/\text{TiO}_2$ catalyst prepared by our research group to explore the impact of tourmaline on its low-temperature SCR catalytic activity.

Previous theoretical and experimental investigation have shown that the combination of denitration catalytic materials and tourmaline with the electric field existing in the rough surface can provide stronger surface adsorption, which makes it easier to adsorb and activate reaction gases. Adsorption is the starting point of the denitration catalytic reaction and the pivotal issue to effective denitration of nitrogen oxides. The photo-catalytic material titanium dioxide, as the carrier of manganese-based denitration catalytic materials, tourmaline and its combination can effectively prevent agglomeration, reduce the average grain size, increase the specific surface area and, then, provide more active sites, which is also the dominant factor affecting the catalytic activity of denitration. At the same time, tourmaline itself possesses permanent electrodes, which can effectively expedite the conversion of manganese ions with different valences, accelerate the transfer of electrons, speed up the occurrence of redox reactions and facilitate the activation of reducing agent. The impurity metal elements, such as iron and magnesium, in tourmaline itself will also improve the active sites of catalytic reactions and the catalytic efficiency.

In this paper, the $\text{MnO}_x/\text{TiO}_2$ catalyst was prepared by co-precipitation from the acid hydrolysis residue of titanium dioxide, produced by the sulfuric acid process. The catalyst was doped with tourmaline of different content and the long-term denitration experiment was carried out. The objective of this paper was studies to reveal the influence mechanism of tourmaline addition on the $\text{MnO}_x/\text{TiO}_2$ catalyst through XRD, BET, NH_3 -TPD (ammonia temperature programmed desorption) and DFT (Density functional theory) calculations. Our findings could provide more ideas for the application of nonmetallic minerals to improve the activity of catalysts.

2. Results and Discussion

2.1. Activity Evaluation of Catalytic Materials

Firstly, the denitration activity of $\text{MnO}_x/\text{TiO}_2$ catalysts with different tourmaline content (0%, 5%, 10% and 20% of Ti total mass) were tested at different reaction temperatures. The change of denitration activity with reaction temperature was measured, as shown in Figure 1.

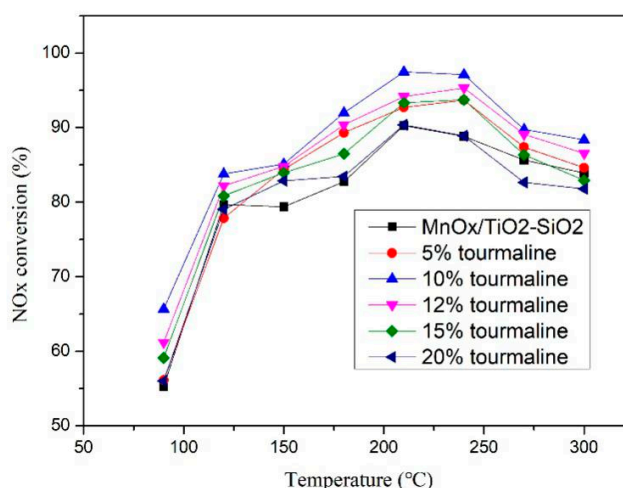


Figure 1. Denitration activity chart of $\text{MnO}_x/\text{TiO}_2$ catalytic materials at different temperatures.

From Figure 1 it can be observed that tourmaline can have a significant improvement on the SCR catalytic performance of $\text{MnO}_x/\text{TiO}_2$ catalytic materials at low temperature. The denitration efficiency of catalytic materials with different tourmaline content varies with temperature. With the increase of reaction temperature, the overall denitration efficiency showed a trend of rising first and then decreasing. The optimum denitration activity temperature of different catalytic materials was about 200 °C, and the efficiency of denitration could reach 97%, which is about 7% higher than that of undoped tourmaline. When the dosage increased to 12%, the denitration activity began to decline and then continued to increase to 15%, with the activity basically consistent with 5% doping. It was concluded that the addition of tourmaline can promote the denitration activity of the catalytic material to a certain extent and the optimum content of tourmaline is 10%. At this moment, the overall catalytic efficiency of the catalytic material reached its highest. However, with the further increase of its dosage, the performance of catalytic materials declined; at some temperatures the denitration rate was lower than that of undoped tourmaline. In order to understand the influence mechanism of tourmaline more intuitively and clearly, and facilitate the subsequent comparison, we chose four typical mixtures (0%, 5%, 10%, 20% hereinafter) for concrete analysis.

2.2. Stability Evaluation of Catalytic Materials

The denitration effect of catalytic materials improved most obviously when the content of tourmaline was 10%; therefore, in the stability evaluation experiment, we compared the denitration rate of catalyst materials before and after adding 10% tourmaline at 200 °C for 10 h, the results are shown in Figure 2.

As shown in Figure 2, the curve of denitration rate for pure $\text{MnO}_x/\text{TiO}_2$ catalyst material presents a steeper slope; however, the overall denitration rate increases with the addition of 10% tourmaline, and the decline rate is slower. For the pure $\text{MnO}_x/\text{TiO}_2$ catalyst, the NO conversion decreased rapidly from 90% to 79% and dropped by 11% within 10 h at 200 °C, while the denitration rate of $\text{MnO}_x/\text{TiO}_2$ catalyst material with 10% tourmaline dropped gradually with time, the performance declined from 97% to 91% and only had a 6% reduction. Therefore, it can be concluded that the addition of tourmaline can effectively slow down the decline of $\text{MnO}_x/\text{TiO}_2$ catalyst material after long-term denitration, prolong the time of denitration duration and improve the stability of the denitration process. In order to comprehend the specific reasons for the above mentioned effects of tourmaline on the denitration activity of catalytic materials, the following methods were characterized and analyzed.

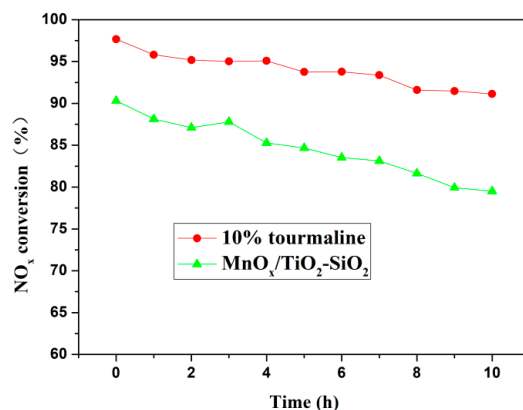


Figure 2. The 200 °C denitrification activity diagram of MnO_x/TiO₂ catalytic materials. Before and after doping with 10% tourmaline.

2.3. Phase Analysis of Catalytic Materials

The existence of various phases in catalytic materials and the completeness of crystallization are important factors affecting their catalytic activity for denitration [8]. In order to understand the effect of tourmaline on the phase form and crystallinity of MnO_x/TiO₂ catalytic materials, XRD measurements of undoped catalytic materials and tourmaline powders were carried out respectively, the results are shown in Figure 3. Through the analysis of XRD spectra of undoped tourmaline MnO_x/TiO₂ catalytic materials, it can be concluded that the principal forms of titanium dioxide as the carrier of catalytic materials are anatase and rutile, with great crystallization. At the same time, the diffraction peaks of Fe₂O₃, SiO₂ and Mn₃O₄ can be detected, but the intensity of XRD peaks is relatively weak. According to the percentage of each chemical component in the acidolysis residue listed in Table 4, it can be seen that most of the components of Fe₂O₃, SiO₂ and Mn₃O₄ still exist in the catalytic materials in the amorphous form. You et al. [9] found that the active component in amorphous state can form –NH₂ by activating NH₄⁺ at the Brownster acidic site, and then react rapidly with NO through the E-R catalytic reaction mechanism to promote the activity of the SCR reaction. Therefore, the component existing in amorphous state is one of the reasons for the high initial denitration activity of MnO_x/TiO₂ catalytic materials, which is consistent with the previous research conclusions of our group. The XRD spectra of tourmaline shows that it is a typical high-purity tourmaline with no other impurities.

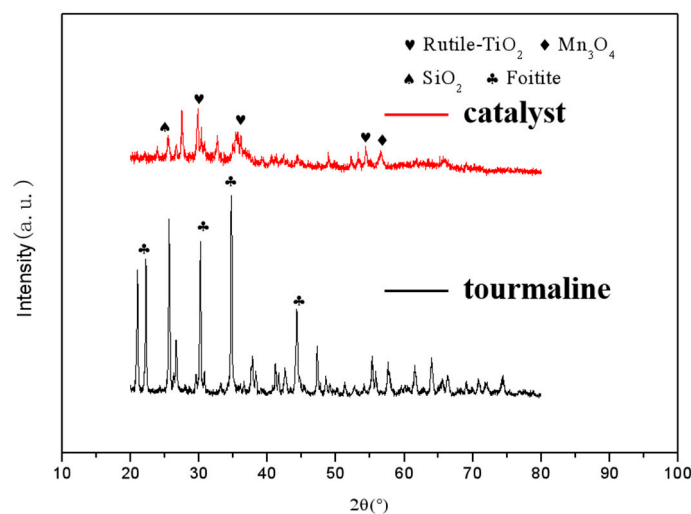


Figure 3. XRD diagrams of tourmaline and MnO_x/TiO₂ catalytic materials.

The XRD spectra of MnO_x/TiO₂ catalytic materials with different tourmaline content is shown in Figure 4. It can be seen from the figure that tourmaline was not consumed during the reaction process,

but was successfully doped into the catalytic materials, and at the same time, the crystallinity of the catalytic materials was affected to varying degrees. As mentioned above, amorphous catalytic materials play a more important role in the denitration reaction, while the tourmaline surface has a strong interaction. Their spontaneous permanent electrodes attract or repel each other. Once successfully incorporated into the catalytic materials, they can effectively promote the dispersion of their powders and then change the crystalline integrity. This is one of the reasons that tourmaline affects the denitration activity of catalytic materials.

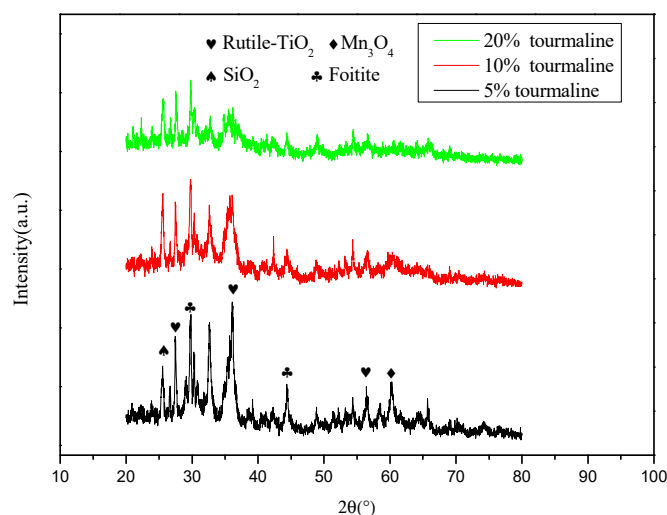


Figure 4. XRD diagram of $\text{MnO}_x/\text{TiO}_2$ catalytic materials with different tourmaline content.

2.4. Analysis of Specific Surface Area and Pore Structure of Catalytic Materials

The specific surface area of catalytic materials affects the distribution of acidic sites; the larger specific surface area means a broader space for the denitration reaction. The denitration activity of catalytic materials can be qualitatively judged by this parameter [10], so it is often regarded as one of the key parameters to be studied. In this section, specific surface area analysis of $\text{MnO}_x/\text{TiO}_2$ catalytic materials with different tourmaline doping amounts is carried out. The parameters of specific surface area, pore size and pore volume of different catalytic materials are listed in Table 1. It can be seen that the specific surface area of the catalytic material before doping with tourmaline is $80.8 \text{ m}^2/\text{g}$, and the pore size and pore volume are 10.1 nm and $23.5 \times 10^{-2} \text{ cm}^3/\text{g}$, respectively. With the increase of tourmaline content, the specific surface area and pore volume of the catalytic material present the same change trend (i.e., increase first and then decrease), but the change of pore size is not obvious. Among them, the specific surface area and pore volume of the catalytic material obtained by 10% tourmaline doping are the optimum, which is also one of the reasons for the best denitration activity of the doped catalytic materials. The results of XRD analysis show that a handful of tourmaline can change the crystallinity of the catalytic material, reduce the agglomeration phenomenon, raise the specific surface area and increase the reaction space on the surface of the catalytic material and the amount of active sites involved in the reaction, so as to improve its denitration activity effectively. However, with the continuous increase of its content, the crystallinity changes and the specific surface area begins to decrease. This is on account of the excessive addition of tourmaline, the enhanced interaction between particles of catalytic materials, the increased probability of collision between particles (resulting in the deepening of agglomeration) and the reduction of the effective utilization of active sites of catalytic materials, so the denitration efficiency decreases more obviously.

Table 1. Specific surface area of MnO_x/TiO₂ with different tourmaline contents.

Sample	S _{BET} / (m ² /g)	Pore Volume / (×10 ⁻² cm ³ /g)	Average Pore Diameter / (nm)
MnO _x /TiO ₂	80.8	23.5	10.1
5% tourmaline	88.3	27.1	10.8
10% tourmaline	98.7	28.1	11.3
20% tourmaline	90.5	25.3	11.1

By contrasting the pore volume of several samples with the corresponding pore size, the particle size distribution of MnO_x/TiO₂ catalytic materials with different tourmaline content was acquired, as shown in Figure 5. Comparing the obtained curves with the existing sixth typical adsorption isotherms, it can be observed that the adsorption isotherms of several catalytic materials belong to type IV. The adsorption–desorption isotherms are inconsistent, which is attributed to the phenomenon of capillary condensation [11,12]. Meanwhile, the hysteresis loop in the diagram belongs to type H1. Their appearance is often related to the type and size of pore structure in the catalytic materials, which means that the channel connectivity between the mesopores of the catalytic materials is very great, and the size of the pore is almost the same. The hysteresis loop also shows that the catalytic materials with different tourmaline content belong to mesoporous structure, and the pore size is between 2 and 50 nm, which corresponds to the results measured by the instrument in Table 1.

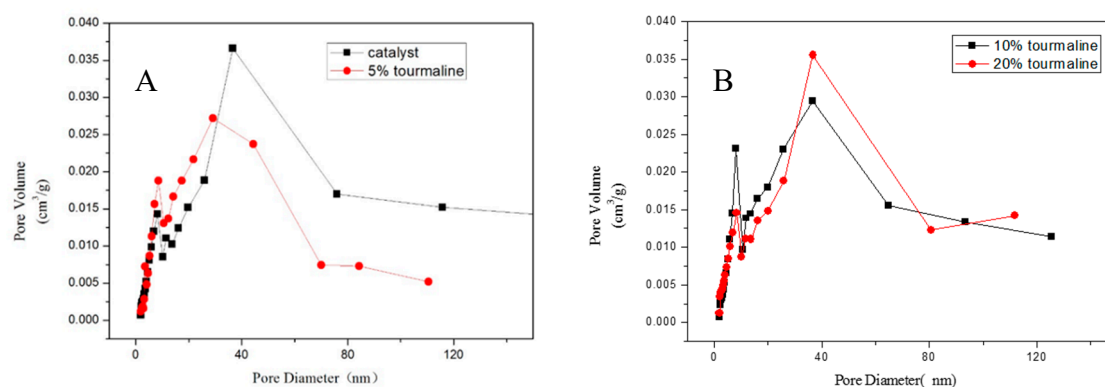


Figure 5. Particle size distribution of MnO_x/TiO₂ catalytic materials with different tourmaline contents. (A): catalyst and 5% tourmaline, (B): 10% tourmaline and 20% tourmaline.

2.5. Surface Acid Sites Analysis of Catalytic Materials

In the process of SCR denitration catalytic reaction, the key step is the adsorption and activation of the reducing agent ammonia, which is also the starting point of the whole reaction. The number of acidic sites on the surface of catalytic materials is the decisive factor. The NH₃-TPD test mainly analyzed and counted the distribution, types and numbers of acid sites on the surface of catalytic materials. Literature studies [13,14] showed that the area and location of the NH₃ desorption peak in the test results could effectively reflect the number and intensity of acid sites.

The experimental results show that the denitration activity and specific surface area of catalytic materials are the maximum when the content of tourmaline is 10%. Therefore, the following work mainly focuses on the performance changes of MnO_x/TiO₂ catalytic materials before and after adding 10% tourmaline. The test results of NH₃-TPD are shown in Figure 6. As shown in the figure, there is only one desorption peak for both catalytic materials before and after doping with tourmaline, which indicates that the intensity distribution of acid sites on the surface of the catalytic materials is concentrated, the desorption peak strength of the 10% tourmaline-doped MnO_x/TiO₂ catalytic material is obviously higher than that before doping and the integral area of the curve can effectively represent the number of acid sites, that is, the addition of tourmaline greatly increased the number of acidic

sites on the surface of the catalytic material. The temperature range of NH_3 desorption is 500~600 °C, which belongs to the high temperature desorption peak. This indicates that NH_3 desorption mainly comes from strong acidic sites on the surface of catalytic materials. According to the denitration rate curves of different catalytic materials in Figure 1, tourmaline can effectively promote the dispersion of catalytic materials, thus increasing the number of acidic sites on the surface of catalytic materials. Therefore making the molecules of reaction gases more easily adsorbed on the surface of catalytic materials and further activated, which is the chief reason for the increase of denitration rate.

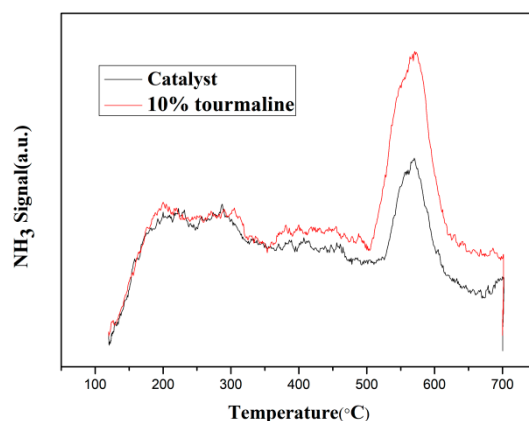


Figure 6. NH_3 -TPD diagram of $\text{MnO}_x/\text{TiO}_2$ catalytic material before and after 10% tourmaline addition.

2.6. Valence State Analysis of Surface Elements of Catalytic Materials

The valence states of the elements in the active components of catalytic materials also affect their denitration activities to a great extent [15,16]. In order to analyze the changes of surface element composition and valence state of $\text{MnO}_x/\text{TiO}_2$ catalytic materials before and after adding tourmaline, XPS analysis was carried out for different catalytic materials. Figure 7 shows the Mn2p XPS spectra of catalytic materials before and after adding 10% tourmaline. It is found that there are two peaks in the spectra. The two main peaks correspond to $\text{Mn}2p_{3/2}$ (641.7 eV) and $\text{Mn}2p_{1/2}$ (653.6 eV), respectively. This indicates that Mn in the catalytic materials exists in various valence states [17]. The measured data can be divided into peaks and fitted by XPS peak software, and the corresponding peaks with different valence manganese ions can be obtained. At the same time, the proportion of different valence manganese ions in catalytic materials can be calculated to facilitate further analysis of the reaction mechanism. The peak of binding energy in 641.5 eV in the figure corresponds to trivalent manganese ions, while the peak of binding energy in 643.4 eV corresponds to tetravalent manganese ions [18].

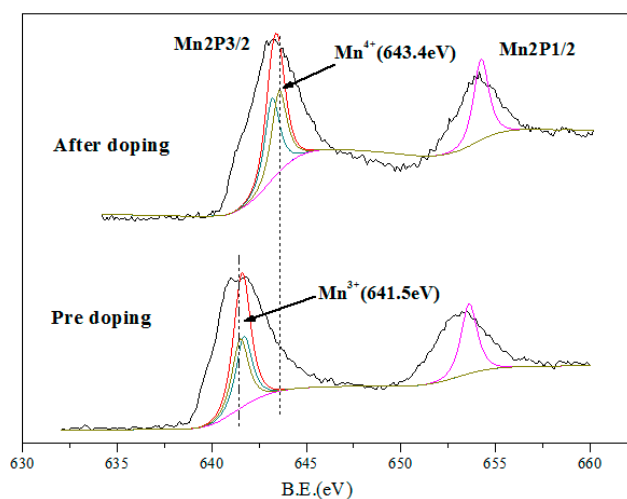


Figure 7. XPS diagram of $\text{MnO}_x/\text{TiO}_2$ catalytic materials before and after 10% tourmaline addition.

According to the content changes of different elements measured in Table 2, it can be concluded that the addition of tourmaline significantly increased the content of MnO_x in catalytic materials, and the valence distribution of manganese ions changed significantly. The content of Mn^{3+} increased relative to that of Mn^{4+} . Literature studies show that the existence of low-valent manganese is more conducive to the adsorption and activation of NO and NH_3 in the catalytic materials, thus promoting the catalytic reaction of denitration and improving the overall denitration efficiency to a certain extent. The addition of tourmaline affects the distribution of manganese ion content in different valence states, which may be owing to the permanent electrode nature of tourmaline itself, which effectively accelerates the transfer of electrons between active components and the oxidation-reduction cycle in the preparation of catalytic materials, improves the process of oxidation-reduction reaction, and then changes the valence distribution of manganese ions in the products and accelerates the occurrence of catalytic reaction.

Table 2. Element contents of $\text{MnO}_x/\text{TiO}_2$ catalytic materials before and after 10% tourmaline addition.

Sample	Element Content (%)				
	MnO_x	$\text{Mn}^{3+}/\text{Mn}^{4+}$	TiO_2	SiO_2	Fe_2O_3
Pre doping	38.77	0.89	16.55	21.06	9.96
After doping	45.35	1.09	11.68	19.54	12.66

2.7. DFT Study

To further study the change of adsorption energy of NO and NH_3 by catalyst after adding tourmaline, we established the model of the catalyst. There is a permanent electrostatic field around tourmaline crystal with the axial plane of C as the two poles [19]. On account of the complex structure of tourmaline, the influence of tourmaline on denitration performance mainly comes from the surface electric field; the doped tourmaline is represented by the applied electric field in Dmol³. After added the electric field, the change of the adsorption energy of the catalyst on the reaction gas was calculated, and its specific influence was explored.

According to the XRD analysis results, the main active component of the catalyst was Mn_3O_4 ; the major carrier was TiO_2 . Therefore, the construction of the catalyst model was selected as $\text{Mn}_3\text{O}_4/\text{TiO}_2$. The obtained geometries for NO and NH_3 molecules adsorbed on the surface of the $\text{Mn}_3\text{O}_4/\text{TiO}_2$ model in the electric field was shown in Figures 8 and 9, respectively. As we can see from the diagram, the NO molecule was inclined to adsorb above the Mn atoms with its N end; the distance between N atom and Mn was 1.727 Å. Simultaneously, the NH_3 molecule was also liable to adsorb above the Mn atoms with its N end; the distance between N atom and Mn was 2.097 Å.

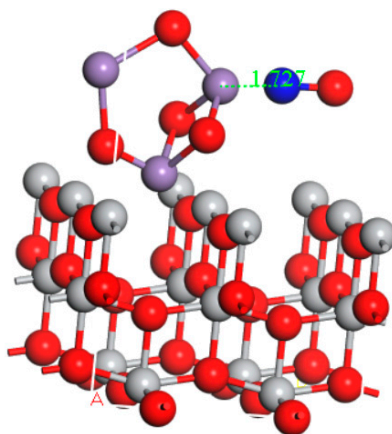


Figure 8. Optimized adsorption structure of NO on the $\text{Mn}_3\text{O}_4/\text{TiO}_2$ model in the electric field.

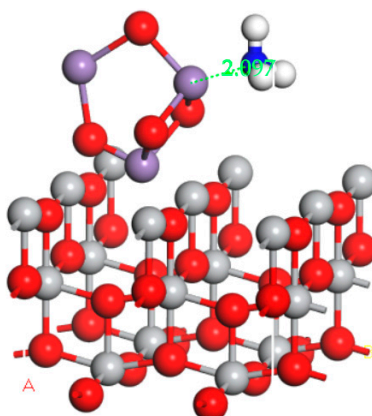


Figure 9. Optimized adsorption structure of NH_3 on the $\text{Mn}_3\text{O}_4/\text{TiO}_2$ model in the electric field.

The adsorption energy for NO and NH_3 on the $\text{Mn}_3\text{O}_4/\text{TiO}_2$ surface were tabulated in Table 3. The E_{ad} values of $\text{Mn}_3\text{O}_4/\text{TiO}_2\text{-NO}$ and $\text{Mn}_3\text{O}_4/\text{TiO}_2\text{-NH}_3$ were calculated as 5.24 and 1.58 eV, respectively, NO molecules were more easily adsorbed on the surface of the catalyst than NH_3 . However, the previous work of the research group shows that the adsorption energy of the catalyst without electric field is 2.66 and 1.38 eV. [20]. The adsorption energy of NO and NH_3 in the presence of an electric field was higher than that in the absence of electric field, indicating that the amount of adsorption of NO and NH_3 were enhanced by the presence of tourmaline; at the same time, the performance of the catalyst was promoted. Electron transfer reaction is the basic step of redox reaction [21], it is also the principle behind how the catalyst works. The spontaneous electric field of tourmaline can speed up proton and electron transfer, increase the degree of electron activation, raise the collision probability between reaction gas and catalyst and then promote the adsorption of NO and NH_3 , ultimately speeding up the chemical reaction rate.

Table 3. Total energy of NO and NH_3 on $\text{Mn}_3\text{O}_4/\text{TiO}_2$.

		Cycle	Total Energy (Ha)	Energy Change	Max Gradient	Max Displacement
$\text{Mn}_3\text{O}_4/\text{TiO}_2$	opt==	63	-2822.276	-0.0000562	0.001697	0.024240
NO	opt==	6	-129.921	-0.0000048	0.000171	0.000048
NH_3	opt==	4	-56.570	-0.0000234	0.000503	0.002988
$\text{Mn}_3\text{O}_4/\text{TiO}_2 + \text{NO}$	opt==	45	-2952.384	-0.0000446	0.001372	0.009183
$\text{Mn}_3\text{O}_4/\text{TiO}_2 + \text{NH}_3$	opt==	15	-2878.904	-0.0000503	0.001845	0.026919

3. Materials and Methods

3.1. Experimental Materials

The selected raw material adopt the acid hydrolysis residue from the process of producing titanium dioxide by sulfuric acid. The chemical composition of the residue and tourmaline are listed in Tables 4 and 5 respectively. The natural tourmaline used in the experiment was mined in Chifeng area, Inner Mongolia, China. It belongs to high-purity natural black tourmaline. The particle size of tourmaline is less than 100 micron. The experimental reagents were manganese acetate ($\text{C}_4\text{H}_6\text{MnO}_4 \cdot 4\text{H}_2\text{O}$), ammonia, 30% hydrogen peroxide, anhydrous ethanol, etc., buy in Beijing Yongng Chemical Co. LTD.

Table 4. The chemical composition of acidolysis residue (mass fraction/%).

%.	TiO_2	SiO_2	SO_3	MnO	Fe_2O_3	CaO
Acid residue	22.2370	34.0827	18.8343	0.9559	8.8500	8.4181

Table 5. The chemical composition of tourmaline (mass fraction/%).

%	B ₂ O ₃	SiO ₂	MgO	Al ₂ O ₃	FeO	Others
Tourmaline	10.08	35.23	4.00	33.55	8.50	8.64

3.2. Catalytic Preparation

MnO_x/TiO₂ catalytic materials were prepared by co-precipitation. The acid residue, after grinding and sieving, was mixed with a certain proportion of manganese acetate at room temperature solution (Mn/Ti = 0.6). Then different proportions of tourmaline (quality accounts for 5%, 10%, 20% of the Ti quality) were added to the mixture solution and magnetic stirred until mixed completely. Ammonia water was used as precipitant, the pH of the solution was controlled to be equal to 11 and hydrogen peroxide was added to the solution until it reached a uniform color. After being centrifugalized and washed, the sample was dried and calcinated at 723 K for 3 h. The final product was the MnO_x/TiO₂ catalytic material.

3.3. Testing Methods and Instruments

The crystal structures of the catalysts were analyzed via X-ray diffraction (XRD) (Shimadzu, Kyoto, Japan) with a Cu K α radiation over a 2 θ range between 20° and 80°. The specific surface area and pore structure of catalytic materials were analyzed by N₂ adsorption and desorption at 350 °C on a TriStar II 3020 high-speed automatic specific surface area and porosity analyzer made by Micromerics Company. NH₃-TPD analysis of catalytic materials was carried out by ChemBET Pulsar TPR/TPD chemisorption analyzer produced by Quantachrome Company (Boynton Beach, FL, USA). The NH₃-TPD detection and analysis process were as follows: The samples of 0.1–0.2 g catalytic materials were pretreated at 550 °C for 1 h, cooled to 120 °C and then high purity NH₃ was introduced. After stabilization for half an hour, the samples were heated to 700 °C at a rate of 10 °C/min. The composition of catalytic materials was quantitatively measured by XRF-1800 sequential X-ray fluorescence spectrometer produced by Shimadzu Company of Japan. ESCALAB250 X-ray photoelectron spectroscopy (XPS) of Thermo Fisher Scientific Company (Waltham, MA, USA) was used to analyze the valence states of the surface elements of the catalytic materials.

The catalytic reaction was carried out on a fixed-bed quartz reactor containing 3 mL catalyst (40–60 mesh). The gas flow rate and the gas hourly space velocity (GHSV) were 1350 mL/min and 27,000 h⁻¹, respectively. The reactant gases contained 1000 ppm NO, 1000 ppm NH₃, 5% O₂ and N₂ balance. The gases were controlled by the Flow controller, and the denitration data were measured at different temperatures 5 min after the reaction gas (NH₃, NO) was injected. The rate of NO_x conversion was calculated according to the follow equation.

$$\text{NO}_x \text{ conversion: } \eta = 100\% \times (1 - [\text{NO}_x]_{\text{out}}/[\text{NO}_x]_{\text{in}})$$

$$[\text{NO}_x] = [\text{NO}] + [\text{NO}_2]$$

[NO_x]_{in}—the concentration of inlet NO_x

[NO_x]_{out}—the concentration of outlet NO_x

3.4. Calculation Details

According to our previous work, we found the cluster model of Mn₃O₄ with the lowest energy and made it the active substance. Titanium dioxide can increase the specific surface area of the catalyst as a carrier and the TiO₂ (001) face shows higher catalytic activity than SiO₂, so we reconstructed it by a (2 × 2) super cell as the carrier model. A vacuum gap of 10 Å aim was used to avoid the interference between different layers. When it is cleaned under vacuum conditions, a 3-layer slab is sufficient to ensure that the calculation will not too big within a certain range of the accuracy requirement because

of its self-driven reconstruction. The bottom two layers were fixed to the bulk parameter during the optimization process.

All the density function theory plus the dispersion (DFT-D) calculation were carried out through Dmol³ in the material studio 2017 (Accelrys, San Diego, CA, USA). The exchange-correlation functional GGA-PW91 and a double numerical basis set with polarization function (DNP), with spin unrestricted, were used. The core treatment was set to effective core potentials (ECPs). The space cutoff radius was maintained at 4.6 Å. The Brillouin zone was sampled by $2 \times 2 \times 1$ k-points using the Monkhorst-Pack scheme. The adsorption energy was calculated according the follow equation:

$$E_{\text{ads}} = E_{\text{cata}} + E_{\text{gas}} - E_{\text{cata-gas}}$$

E_{cata} —the total energy of the model of $\text{MnO}_x/\text{TiO}_2$ catalyst, E_{gas} —the total energy of free gas molecule, $E_{\text{gas}} - E_{\text{cata-gas}}$ —the total energy of the model of that gas adsorbed on the $\text{MnO}_x/\text{TiO}_2$ catalyst. Note that positive value for E_{ads} indicated a strong interaction between the adsorption substrate and gas.

4. Conclusions

In this paper, $\text{MnO}_x/\text{TiO}_2$ catalytic materials were obtained by coprecipitation method from acid hydrolysis residue of titanium dioxide, produced by the sulfuric acid process. The impact of tourmaline doping on the denitration performance of the $\text{MnO}_x/\text{TiO}_2$ catalytic material was analyzed, the conclusions are as follows:

The adjunction of tourmaline can improve the catalytic performance of $\text{MnO}_x/\text{TiO}_2$ catalytic material at low temperature with the optimum tourmaline content of 10%. At this point, the specific surface area of the catalytic material achieves the maximum level, the overall denitration activity reaches the best, and the catalytic efficiency can achieve 97%. With the further increase of its dosage, the interaction between particles strengthens, which leads to aggravation of agglomeration and an obvious decrease of the denitration rate.

The permanent electrode property of tourmaline itself can effectively promote the dispersion of $\text{MnO}_x/\text{TiO}_2$ catalytic materials, increase the number of acidic sites on its surface, make it easier to adsorb and activate reactant molecules and, finally, improve the denitration efficiency. At the same time, tourmaline could effectively change the valence distribution of manganese ions in the products, promote the transfer of proton and electrons, increase the collision probability between reaction gas and catalyst, speed up the process of redox reaction and, then, improve the catalytic performance.

Author Contributions: Funding acquisition, Methodology, S.C.; Supervision, X.M.; Writing—original draft, Y.H. All authors have read and agreed to the published version of the manuscript.

Funding: This research was funded by the National Key R&D Program of China (Approval No. 2017YFB0310802) and the Foundation for Innovative Research Groups of the National Natural Science Foundation of China (Approval No. 51621003).

Conflicts of Interest: The authors declare no conflict of interest.

Abbreviations

The following abbreviations are used in this manuscript:

SCR	Selective Catalytic Reduction
DFT	Density Functional Theory

References

1. Li, X. Optimization and reconstruction technology of SCR flue gas denitrification ultra low emission in coal fired power plant. *IOP Conf. Ser. Mater. Sci. Eng.* **2017**, *231*, 012111. [[CrossRef](#)]
2. Hu, Y.-F.; Bai, Y.-F. SCR denitration Technology and its Application. *Energy Conserv. Technol.* **2007**, *25*, 152–156.

3. Johannessen, T.; Koutsopoulos, S. One-Step Flame Synthesis of an Active Pt/TiO₂ Catalyst for SO₂ Oxidation—A Possible Alternative to Traditional Methods for Parallel Screening. *J. Catal.* **2002**, *205*, 404–408. [[CrossRef](#)]
4. Zhuang, K.; Zhang, Y.; Huang, T.; Lu, B.; Shen, K. Sulfur-poisoning and thermal reduction regeneration of holmium-modified Fe-Mn/TiO₂ catalyst for low-temperature SCR. *J. Fuel Chem. Technol.* **2017**, *45*, 1356–1364. [[CrossRef](#)]
5. Dunn, P.J.; Appleman, D.; Nelen, J.A.; Norberg, J. Uvite, a new (old) common member of the tourmaline group and its implications for collectors. *Mineral. Rec.* **1977**, *8*, 100–108.
6. Ruan, D.; Zhang, L.; Zhang, Z.; Xia, X. Structure and properties of regenerated cellulose/tourmaline nanocrystal composite films. *J. Polym. Sci. Part B Polym. Phys.* **2004**, *42*, 367–373. [[CrossRef](#)]
7. Huang, F.; Guo, Y.; Wang, S.; Zhang, S.; Cui, M. Solgel-hydrothermal synthesis of Tb/Tourmaline/TiO₂ nano tubes and enhanced photocatalytic activity. *Solid State Sci.* **2017**, *64*, 62–68. [[CrossRef](#)]
8. Liu, F.; He, H.; Xie, L. XAFS Study on the Specific Deoxidation Behavior of Iron Titanate Catalyst for the Selective Catalytic Reduction of NO_x with NH₃. *ChemCatChem* **2013**, *5*, 3760–3769. [[CrossRef](#)]
9. Chen, L.; Li, J.; Ge, M.; Zhu, R. Enhanced activity of tungsten modified CeO₂/TiO₂ for selective catalytic reduction of NO_x with ammonia. *Catal. Today* **2010**, *153*, 77–83. [[CrossRef](#)]
10. Won, J.M.; Kim, M.S.; Hong, S.C. Effect of vanadium surface density and structure in VO_x/TiO₂ on selective catalytic reduction by NH₃. *Korean J. Chem. Eng.* **2018**, *35*, 2365–2378. [[CrossRef](#)]
11. Michalow-Mauke, K.A.; Lu, Y.; Kowalski, K.; Graule, T.; Nachttegaal, M.; Kröcher, O.; Ferri, D. Flame-Made WO₃/CeO_x-TiO₂ Catalysts for Selective Catalytic Reduction of NO_x by NH₃. *ACS Catal.* **2015**, *5*, 5657–5672. [[CrossRef](#)]
12. Yao, X.; Zhao, R.; Chen, L.; Du, J.; Tao, C.; Yang, F.; Dong, L. Selective catalytic reduction of NO_x by NH₃ over CeO₂ supported on TiO₂: Comparison of anatase, brookite, and rutile. *Appl. Catal. B Environ.* **2017**, *208*, 82–93. [[CrossRef](#)]
13. Xia, F.; Song, Z.; Liu, X.; Liu, X.; Yang, Y.; Zhang, Q.; Peng, J. Improved catalytic activity and N₂ selectivity of Fe–Mn–O_x catalyst for selective catalytic reduction of NO by NH₃ at low temperature. *Res. Chem. Intermed.* **2018**, *44*, 2703–2717. [[CrossRef](#)]
14. Qi, K.; Xie, J.; Mei, D.; He, F.; Fang, D. The utilization of fly ash-MnO_x /FA catalysts for NO_x removal. *Mater. Res. Express* **2018**, *5*, 065526. [[CrossRef](#)]
15. Huang, J.; Huang, H.; Liu, L.; Jiang, H. Revisit the effect of manganese oxidation state on activity in low-temperature NO-SCR. *Mol. Catal.* **2018**, *446*, 49–57. [[CrossRef](#)]
16. Lian, Z.; Shan, W.; Zhang, Y.; Wang, M.; He, H. Morphology-Dependent Catalytic Performance of NbO_x/CeO₂ Catalysts for Selective Catalytic Reduction of NO_x with NH₃. *Ind. Eng. Chem. Res.* **2018**, *57*, 12736–12741. [[CrossRef](#)]
17. Meng, B.; Zhao, Z.; Chen, Y.; Wang, X.; Li, Y.; Qiu, J. Low-temperature synthesis of Mn-based mixed metal oxides with novel fluffy structures as efficient catalysts for selective reduction of nitrogen oxides by ammonia. *Chem. Commun.* **2014**, *50*, 12396–12399. [[CrossRef](#)]
18. Lai, X.; Roberts, K.J.; Avanci, L.H.; Cardoso, L.P.; Sasaki, J.M. Habit modification of nearly perfect single crystals of potassium dihydrogen phosphate (KDP) by trivalent manganese ions studied using synchrotron radiation X-ray multiple diffraction in Renninger scanning mode. *J. Appl. Crystallogr.* **2003**, *36*, 1230–1235. [[CrossRef](#)]
19. Rui-Hua, W.U.; Yun-Hui, T.; Xiao-Hui, Z. The Electrostatic Field Effect of Tourmaline Particles and the Prospect of Its Application to Environmental Protection Field. *Acta Petrol. Mineral.* **2001**, *20*, 474–476.
20. Wei, L.; Cui, S.; Guo, H.; Zhang, L. The effect of alkali metal over Mn/TiO₂ for low-temperature SCR of NO with NH₃ through DRIFT and DFT. *Comput. Mater. Sci.* **2018**, *144*, 216–222. [[CrossRef](#)]
21. Zhao, F.; Zhang, J.; Kaneko, M. Electron transfer in the redox reaction of cobalt tetraphenylporphyrin incorporated in a Nafion film. *J. Porphy. Phthalocyanines* **2000**, *4*, 158–167. [[CrossRef](#)]

